2018 European Control Conference (ECC)
June 12-15, 2018. Limassol, Cyprus

Iterative Learning Control with Bézier Curve-Based Corner Smoothing for Feed Drive Systems*

Kenneth Renny Simba[1], Gunter Heppeler[1,2], Hiroaki Noguchi[1], Oliver Sawodny[2] and Naoki Uchiyama[1]

Abstract— **Feed drive systems play an important role in manufacturing industries owing to their wide range of applications. This study proposes a simple iterative learning control algorithm and a method to generate smooth and velocity optimal trajectories for feed drive systems. Corners are smoothed through the insertion of fifth order Bézier curves that lead to continuous-curvature trajectories. For performance evaluation, simulations and experiments were conducted with linear and smoothed trajectories. Based on the proposed approach, experimental results showed that the maximum contour error and the control input could respectively be reduced by about 61.5 % and 8.0 % in comparison to traditional approaches.**

I. INTRODUCTION

Feed drive systems particularly machine tools are becoming more popular due to their wide range of use in manufacturing industries. Owing to the increasing demand of precise products, computer numerical control machine tools must operate at high speeds while maintaining high positioning accuracy. For high-speed performance, machine tools need high velocity capabilities, fast controllers under time-optimal trajectories, and lightweight mechanical systems. On the contrary, to ensure high positioning accuracy, one requires stiff systems with accurate motion controllers under slow trajectories. Also, trajectories are required to describe paths accurately, be smooth kinematically and satisfy the physical limitations of machine tools. On the other hand, lightweight mechanical systems operating at high speeds may suffer from significant vibration problems, thus degrading positioning accuracy and exhibiting large settling times [1], [2].

The growing demand for solutions to achieve higher-speed operations while maintaining machining precision has attracted the attention of many researchers from the academic and the industrial communities and is the key driver to the contents of this study.

Many control algorithms including traditional feedback controllers that can achieve high-tracking bandwidth with disturbance rejection have been proposed in the literature [3]–[7]. Most of these traditional controllers require high control gains to achieve the desired performance. However, high gains can destabilise control systems and have several limitations owing to the hardware properties. Furthermore, because it is not always possible to achieve the desired tracking performance based on general control theory due to the presence of unmodelled dynamics and nonlinear uncertainties, intelligent controllers are required to enhance the tracking performance. From the fact that machine tools perform repetitive operations over a fixed time interval, Iterative Learning Control (ILC) can be used as an effective tool to improve transient response and tracking performance. ILC is among the intelligent controllers that imitate the human learning process and is proven to enhance the performance of uncertain dynamical systems [8]–[10]. Although ILC has been widely applied to feed drive systems by regulating the control input, the desired performance can hardly be achieved under discontinuous reference trajectories, for example, in the case that the reference trajectories are not kinematically smooth and do not satisfy physical limitations of feed drive systems. In particular, at high curvatures, an infinite acceleration may be required to achieve a desired tracking performance.

Regarding trajectories, smoothing of linear interpolated tool-path points using curve fitting techniques is among the common methods that are widely applied in machine tools. This includes quadratic, cubic and in rare cases quintic spline curves are used to generate smooth trajectories [11]–[13]. Because high-order spline curves are numerically unstable, if curve fitting methods are applied at densely tool-path points, it leads to oscillations in the trajectory [14], [15]. Therefore, some recent studies proposed interpolation of tool-path points and corner blending using parametric spline curves [15]–[17].

This study proposes a simple iterative learning contouring control approach for feed drive systems. Contouring control is applied owing to its ability to achieve better performance than tracking-error based controllers and in most cases it exhibits smaller control inputs [18]. In addition, this study proposes a method to generate smooth motion trajectories for feed drive systems for a specified error tolerance in a reference contour. The generated trajectory considers fundamental criteria, namely, velocity, acceleration and jerk limits. This trajectory can be tracked easily by a feed drive system and renders a smaller maximum contour error compared to conventional linearly interpolated trajectories.

The rest of this paper is organised as follows: Section II introduces the system dynamics and contouring controller design. The proposed method to generate smooth trajectories is described in section III followed by simulation and experimental results in section IV. Finally, the concluding remarks are summarised in section V.

*This work was partially supported by the Machine Tool Technologies Research Foundation, CA, USA and Magnescale Co. Ltd., Kanagawa, Japan.

[1]The authors are with the Faculty of Mechanical Engineering, Toyohashi University of Technology, 441-8580 Toyohashi, Japan. uchiyama@tut.jp

[2]The authors are with the Institute of System Dynamics, University of Stuttgart, Waldburgsraße 17/19, D-70459 Stuttgart, Germany.

II. CONTROLLER DESIGN

A. Plant Dynamics

The dynamics of a typical feed drive system is represented by the following decoupled second order system:

$$M\ddot{x}+C\dot{x}+F_c\mathrm{sgn}(\dot{x})=K_f i_a, \tag{1}$$

with

$$\begin{aligned}&M=\mathrm{diag}\{m_i\},\quad C=\mathrm{diag}\{c_i\},\\&F_c=\mathrm{diag}\{f_{ci}\},\quad K_f=\mathrm{diag}\{k_{fi}\},\\&x=\begin{bmatrix}x_1 & x_2\end{bmatrix}^{\mathrm{T}},\quad i_a=\begin{bmatrix}i_{a1} & i_{a2}\end{bmatrix}^{\mathrm{T}},\\&i=1,2,\end{aligned}$$

where m_i, x_i, c_i, f_{ci}, k_{fi} and i_{ai} are the equivalent mass of the table, the position of the table, the viscous friction coefficient, Coulomb friction force, force–current conversion ratio and the input voltage to the i^{th} drive axis, respectively.

B. Definition of Contour Error

The contour error is derived from the individual drive axes tracing errors as shown in Fig. 1 [9], [19]. It is the shortest distance between the actual position and the desired contour. In contrast, the tracking error is the difference between the desired and actual positions of each drive axis. The tracking error in each drive axis in coordinate frame Σ_w is defined as

$$e_w=\begin{bmatrix}e_{w1} & e_{w2}\end{bmatrix}^{\mathrm{T}}=x_d-x, \tag{2}$$

where x_d and x represents the desired and the actual positions at sampling instant t. The coordinate frame Σ_l is attached at x_d and its axis directional vectors are $\mathscr{T}$ and $\mathscr{N}$, which are tangential and orthogonal to the reference position x_d, respectively. Thus, the tracking error vector e_w can be expressed with respect to Σ_l as

$$e_l=\begin{bmatrix}e_t & e_n\end{bmatrix}^{\mathrm{T}}=R^{\mathrm{T}}e_w,\quad R=\begin{bmatrix}\cos\theta & -\sin\theta\\ \sin\theta & \cos\theta\end{bmatrix}, \tag{3}$$

where θ is the inclination of Σ_l to Σ_w.

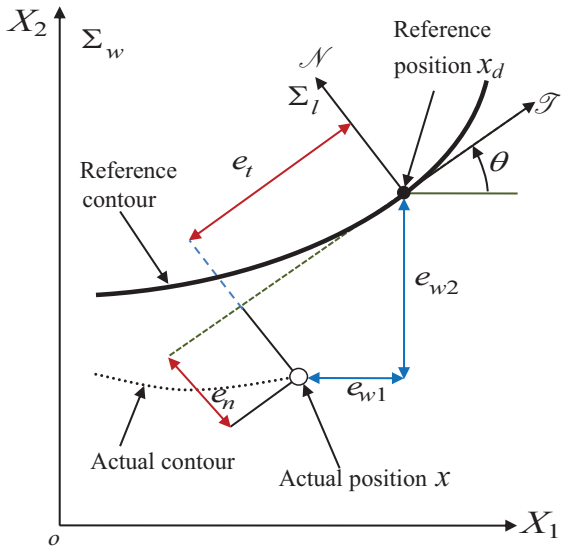

Fig. 1: Definition of tracking and contour errors.

C. Feedback Controller Design

Owing to the nonlinear term in (1), the system is transformed as follows in order to apply linear controllers:

$$\begin{aligned}&z_1=x,\\&z_2=\dot{z}_1,\\&\dot{z}_2=M^{-1}\left(K_f i_a-Cz_2-F_c\mathrm{sgn}(z_2)\right).\end{aligned} \tag{4}$$

The control input

$$i_a=K_f^{-1}\left(Mv+Cz_2+F_c\mathrm{sgn}(z_2)\right), \tag{5}$$

leads to

$$\dot{z}_2=v. \tag{6}$$

The variable $v=\begin{bmatrix}v_1 & v_2\end{bmatrix}^{\mathrm{T}}$ is the virtual input designed as

$$\begin{aligned}&v=\ddot{x}_d+R\left(K_P e_l+K_D\dot{e}_l\right)+\ddot{\theta}\Xi e_w-\dot{\theta}^2 e_w+2\dot{\theta}\Xi\dot{e}_w,\\&K_P=\mathrm{diag}\{k_{Pi}\},\ K_D=\mathrm{diag}\{k_{Di}\},\\&\Xi=\begin{bmatrix}0 & 1\\ -1 & 0\end{bmatrix},\end{aligned} \tag{7}$$

for contouring control [18], where k_{Pi} and k_{Di} are position and velocity feedback (FB) gains, respectively.

D. Application of Iterative Learning Contouring Control

The proposed control system includes the FB to form a control loop with previous and current signal cycles [19]. The axes are coupled by the rotation matrix R, which transforms the tracking error of each drive axis into the contour error. Although both the tangential and the normal components of the error e_t and e_n, respectively, are used in the FB, only the normal component is used in the iterative learning function L_i. This is because L_i aims to converge the actual contour to the desired one. Elements of the normal error e_n regarding each drive axis can be represented as

$$\begin{aligned}&e_{vn}=R_n e_w,\\&R_n=\begin{bmatrix}-\sin^2\theta & \sin\theta\cos\theta\\ -\sin\theta\cos\theta & \cos^2\theta\end{bmatrix}.\end{aligned} \tag{8}$$

Because of the FB controller and the use of contour error instead of tracking error the update law is represented follows:

$$\begin{aligned}&v_{j+1}(t)=Q(b^{-1})\left[v_j(t)+L(b^{-1})e_{vnj}(t)\right]+Ke_{lj+1}(t),\\&Q=\mathrm{diag}\{q_i\},\ L=\mathrm{diag}\{L_i\},\ K=\mathrm{diag}\{K_i\},\end{aligned} \tag{9}$$

where K_i and v_j are the FB gain matrix for axis i and the system control input in the j^{th} iteration. The corresponding error terms $e_{vnj}(t)$ and $e_{lj+1}(t)$ are given by

$$\begin{aligned}&e_{vnj}(t)=R_n\left(x_d(t)-x_j(t)\right),\\&e_{lj+1}(t)=R^{\mathrm{T}}\left(x_d(t)-x_{j+1}(t)\right),\end{aligned} \tag{10}$$

where the reference trajectory x_d remains unchanged iteratively. A variable PID learning function is proposed so that,

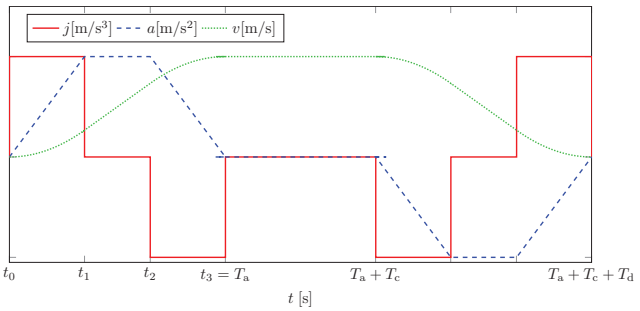

Fig. 2: Example for a jerk limited acceleration profile(JLAP).

the update law at sampling instant t can be written as follows:

$$\begin{aligned} v_{j+1}(t) = {} & Q(b^{-1})v_j(t) + K_P e_{lj+1}(t) + K_D \dot{e}_{lj+1}(t) \\ & + Q(b^{-1})\Psi_{Pj}K_{PL}e_{vnj}(t) \\ & + Q(b^{-1})\Psi_{Ij}K_{IL}\sum_{t=1}^{T} e_{vnj}(t-1) \\ & + Q(b^{-1})\Psi_{Dj}K_{DL}\left\{e_{vnj}(t) - e_{vnj}(t-1)\right\}, \\ K_{mL} = {} & \mathrm{diag}\{k_{mLi}\},\ \Psi_{mj} = \mathrm{diag}\{\psi_{mij}\},\quad m = P,\ I,\ D, \\ \psi_{mij} = {} & 1 - \frac{1}{\alpha_{mi}}\mathrm{sat}\left(\frac{e_{vnij}}{\beta_{mi}}\right),\ 0 \le t \le T-1, \end{aligned} \tag{11}$$

where k_{mLi}, T and b^{-1} are gains of the learning function L_i, the total number of sampling instants and a delay operator, respectively. ψ_{mij} is an error-dependent function with constants $\alpha_{mi} > 0$ and $\beta_{mi} > 0$.

III. SMOOTH TRAJECTORY GENERATION

In order to efficiently generate optimal trajectories, a convenient representation of the trajectory has to be chosen. As many contours can be represented by piecewise linear paths, this representation is chosen in this research. On the linear sections, velocities are described by jerk limited acceleration profiles (JLAPs). In JLAPs, accelerations and decelerations are divided into three segments: in the first and the last segments a constant jerk is applied to increase or decrease the acceleration and in the middle segment the acceleration is kept constant. The accelerations and decelerations start and end with zero magnitude and can be connected by constant velocity sections. An example of a JLAP is shown in Fig. 2. The JLAP gives continuous velocity and acceleration profiles and can be fully described by its length Δs, initial velocity v_0, maximum velocity v_c, end velocity v_e, maximum admissible accelerations, decelerations and jerks, a_a, a_d and j, respectively.

The connection of the linear segments either results in contour errors, due to instantaneous changes in velocity which exceed the machine tools limitations, or requires a full stop at every corner. In order to avoid these limitations, corner smoothing based on fifth-order Bézier curves as proposed in [16] and illustrated in Fig. 3 is used to connect the linear segments.

These Bézier curves have the form

$$\begin{aligned} p = {} & (1-h)^5 p_1 + 5h(1-h)^4 p_2 + 10h^2(1-h)^3 p_3 \\ & + 10h^3(1-h)^2 p_4 + 5h^4(1-h)p_5 + h^5 p_6, \end{aligned} \tag{12}$$

where $h \in [0,1]$ is a dimensionless parameter and p_1 to p_6 are the Bézier curve control points. This allows a smooth blending of the acceleration at the connection of linear and corner segments. Reference [16] proposes a constant path velocity v on the Bézier curve as well as a fixed ratio of length between Bézier points and G_i as shown in Fig. 3. The main design parameter for the Bézier curve in their work is the length ratio $n = l_1/l_2$.

For a given corner angle θ, the relation between the maximum allowed corner error ε and the length $l_t = 2l_1 + l_2$ between p_1 and G_1 is as follows

$$\varepsilon = \frac{(7n+16)\sqrt{2+2\cos\theta}}{64n+32} l_t. \tag{13}$$

The fixed path velocity v leads to the acceleration

$$a = v\frac{\partial}{\partial t}\mu_T = v\frac{\partial}{\partial t}\left(\frac{1}{\left|\frac{\partial p}{\partial h}\right|}\frac{\partial p}{\partial h}\right) = v^2\kappa\mu_N, \tag{14}$$

where μ_T and μ_N are the tangent and the normal vectors of p and κ is the curvature. Since κ can be explicitly expressed by h, n, l_t and θ, the maximum corner velocity due to acceleration limits is found by evaluating

$$v_{\max,a} = \min_h \sqrt{\frac{a_{\max}}{\kappa}}. \tag{15}$$

Therefore, the optimal length ratio n_{opt,l_t} for maximizing the velocity with respect to a given corner and acceleration limit is calculated by solving the optimization problem

$$n_{\mathrm{opt},l_t} = \arg\min_n \left(\max_h \kappa\right). \tag{16}$$

Note that $\kappa \sim 1/l_t$, and therefore in [16], n_{opt,l_t} is determined numerically by setting $l_t = 1$. The cornering error is satisfied by scaling the resulting κ afterwards. However, due to the nonlinear relationship between l_t and ε, given in (13), their method does not yield a maximum velocity with respect to ε. Therefore, here (13) is included in the calculation of κ leading to $\kappa \sim 1/\varepsilon$. The resulting optimal length ratio is referred to as $n_{\mathrm{opt},a}$.

Another point, which was not addressed in [16], is limiting the velocity according to the jerk limit. The absolute value of the jerk is given by

$$j = \left|\frac{\partial}{\partial t}a\right| = \left|\frac{\partial}{\partial t}v^2\kappa\mu_N\right| := v^3\varkappa, \tag{17}$$

with

$$\varkappa = \left|\frac{\frac{\partial p}{\partial h}H_1 + \frac{\partial^2 p}{\partial h^2}H_2 + \frac{\partial^3 p}{\partial h^3}H_3}{\left|\frac{\partial^2 p}{\partial h^2}\right|^7}\right|$$

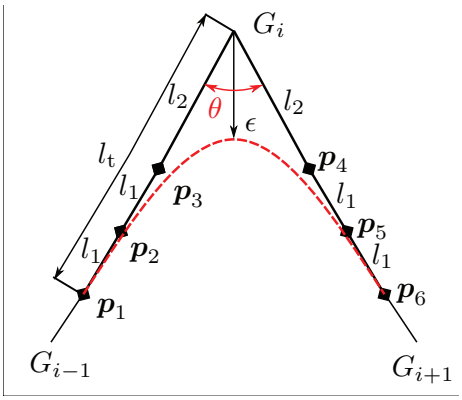

Fig. 3: Corner smoothing by Bézier curves.

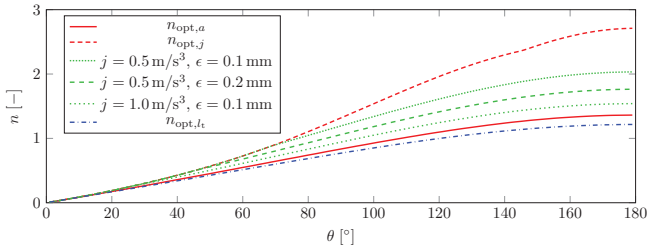

Fig. 4: Optimal values of n with respect to κ and $\dot{\kappa}$ for different sets of a, j and ε. Note that a is $30\,\mathrm{mm\,s^{-2}}$ for all these sets. Also n_{opt,l_t} proposed in [16] is shown.

and

$$H_1 = 4\left(\frac{\partial^2 p}{\partial h^2}^T \frac{\partial p}{\partial h}\right)^2 - \left|\frac{\partial^2 p}{\partial h^2}\right|^2 \left|\frac{\partial p}{\partial h}\right|^2 + \frac{\partial^3 p}{\partial h^3}^T \frac{\partial p}{\partial h}\left|\frac{\partial p}{\partial h}\right|^2,$$

$$H_2 = 3\frac{\partial^2 p}{\partial h^2}^T \frac{\partial p}{\partial h}\left|\frac{\partial p}{\partial h}\right|^2, \quad H_3 = \left|\frac{\partial p}{\partial h}\right|^4.$$

Here $\varkappa \sim 1/\varepsilon^2$ holds. This leads to

$$v_{\max,j} = \min_h \sqrt[3]{\frac{j_{\max}}{\varkappa}} \tag{18}$$

$$n_{\mathrm{opt},j} = \arg\min_n \left(\max_h \varkappa\right). \tag{19}$$

The maximum admissible velocity is the minimum of $v_{\max,a}$ and $v_{\max,j}$, and therefore the optimal length ratio is

$$n_{\mathrm{opt}} = \arg\max_n \min\left(v_{\max,a}, v_{\max,j}\right). \tag{20}$$

Fig. 4 shows a comparison between $n_{\mathrm{opt},a}$, $n_{\mathrm{opt},j}$, n_{opt} for different settings and n_{opt,l_t} as proposed in [16]. It can be seen that n_{opt} is always between $n_{\mathrm{opt},a}$ and $n_{\mathrm{opt},j}$, and n_{opt,l_t} is always slightly smaller than $n_{\mathrm{opt},a}$.

In order to calculate the duration for the smoothed corner, the arc length s_{arc} of the Bézier curve is required. Calculating the arc length analytically by solving the integral

$$s_{\mathrm{arc}} = \int_0^1 \left|\frac{\partial p(h,n,\theta,\varepsilon)}{\partial h}\right| \mathrm{d}h \tag{21}$$

is not possible for fifth-order Bézier curves, and therefore a sixth-order numerical method proposed in [20] is used. The

TABLE I: Plant and controller parameters.

Par.	Unit	x_1	x_2	Par.	Unit	x_1, x_2
m_i	$\mathrm{N\,s^2\,mm^{-1}}$	0.088	0.097	k_{PLi}	$\mathrm{A\,mm^{-1}}$	200
c_i	$\mathrm{N\,s\,mm^{-1}}$	0.559	0.796	k_{ILi}	$\mathrm{A\,s^{-1}\,mm}$	0.2
f_{ci}	N	48	58	k_{DLi}	$\mathrm{A\,s\,mm^{-1}}$	10
k_{fi}	$\mathrm{N\,A^{-1}}$	235.62	331.12	α_{mi}		30
k_{Pi}	$\mathrm{A\,mm^{-1}}$	70000	70000	β_{mi}	mm	0.005
k_{Di}	$\mathrm{A\,s\,mm^{-1}}$	240	240	q_1		1

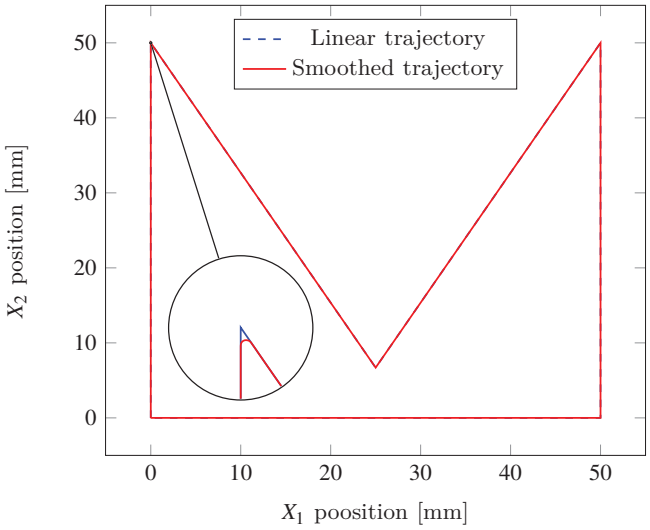

Fig. 5: Reference trajectories for simulation and experiment.

connection point between the linear and corner segments has to be determined before the optimization. However, since l_t varies with n and ε, a conservative selection of the length of the sides l_s of the unilateral triangle, used as corner segment, has to be made. Since, according to (13), l_t increases with n for $n \geq 0$, the highest value of l_t for fixed θ and ε is at the highest value of n, which corresponds to $n_{\mathrm{opt},j}$. This leads to

$$l_s = l_t(n_{\mathrm{opt},j}, \theta, \varepsilon) \tag{22}$$

$$\Delta s = 2\left(l_s - l_t(n_{\mathrm{opt}}, \theta, \varepsilon)\right) + s_{\mathrm{arc}}(n_{\mathrm{opt}}, \theta, \varepsilon). \tag{23}$$

IV. RESULTS

A. Experimental Setup

To evaluate the performance of both the ILC and trajectory smoothing algorithms, a trajectory with 30 deg, 60 deg and 90 deg angles was used for simulation and experiment as shown in Fig. 5. For the smoothed trajectory, the induced geometrical error ε at corners was fixed to 50 µm. A constant velocity of $50\,\mathrm{mm\,s^{-1}}$ was used. For the smoothed trajectory, the velocity was automatically reduced at corners.

B. Simulation Results

Fig. 6 shows simulation results for contour error. In both trajectories, the FB refers to the feedback controller in (7), where as the ILC refers to the iterative contouring controller in (11). The maximum contour error based on the linear trajectory could be reduced by 9 % only, that is from 97.74 µm to 88.92 µm. The application of smoothed

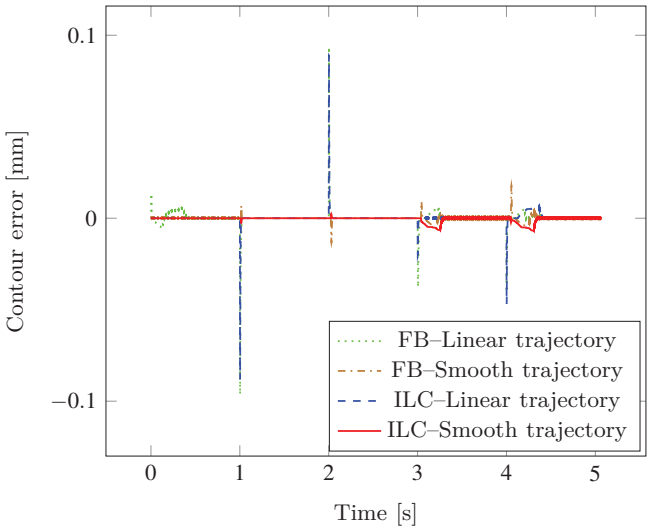

Fig. 6: Simulation results of contour error.

Fig. 7: Experimental feed drive system.

trajectory drastically reduced the maximum contour error to 17.78 µm, which is about 82 % compared to the linear trajectory. By adding the ILC, the error was reduced to 6.88 µm, which is equivalent to 61.3 %. The ILC achieved higher percentage of maximum contour error reduction based on the smoothed trajectory than the linear one. As stated in section I, high curvature may lead to saturation of control inputs and therefore no further control can be done at a particular curvature.

C. Experimental Results

An experiment was done on an industrial biaxial feed drive system in Fig. 7. For both the linear and smoothed trajectory, the feedback controller in (7) was used. Fig. 8 shows the contour error for both trajectories followed by their corresponding individual drive axes tracking errors in Figs. 9 and 10. The maximum contour error based on the linear trajectory was 0.31 mm, and was reduced to 0.11 mm after applying the smoothing algorithm. This is equivalent to a reduction of 61.52 % of the maximum contour error. Also, the average contour error was reduced by 60.25 %.

Fig. 11 shows the velocities for both trajectories and their corresponding control forces in Fig. 12. Although the

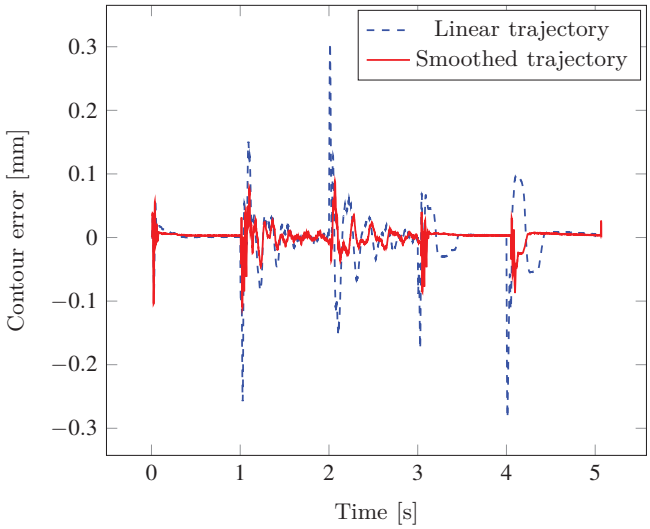

Fig. 8: Experimental contour error.

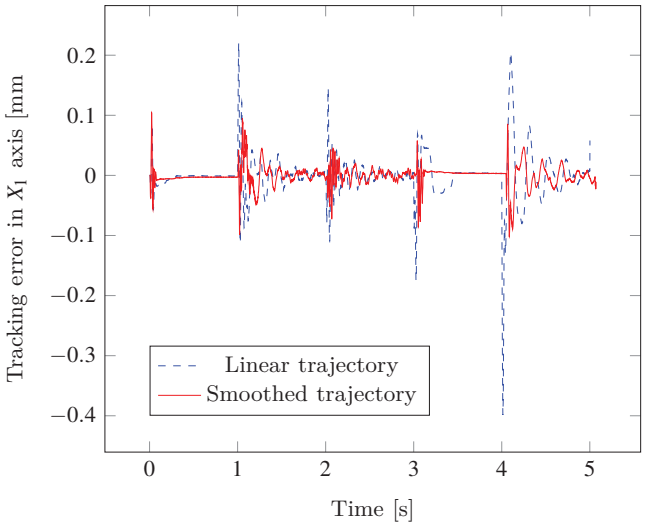

Fig. 9: Experimental tracking error in X_1 axis.

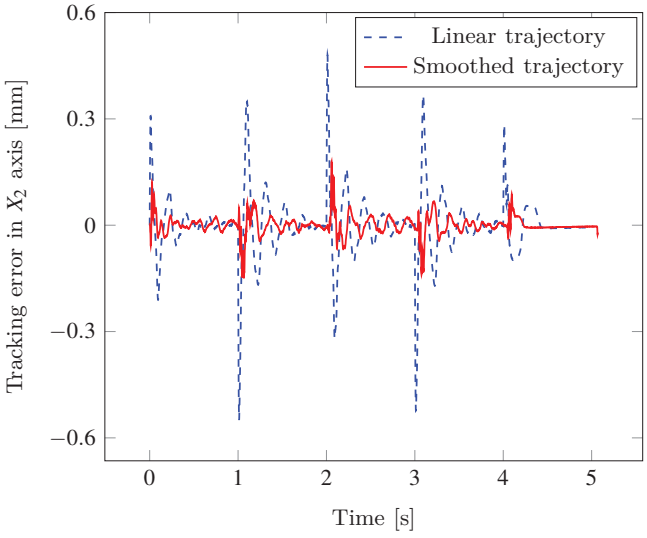

Fig. 10: Experimental tracking error in X_2 axis.

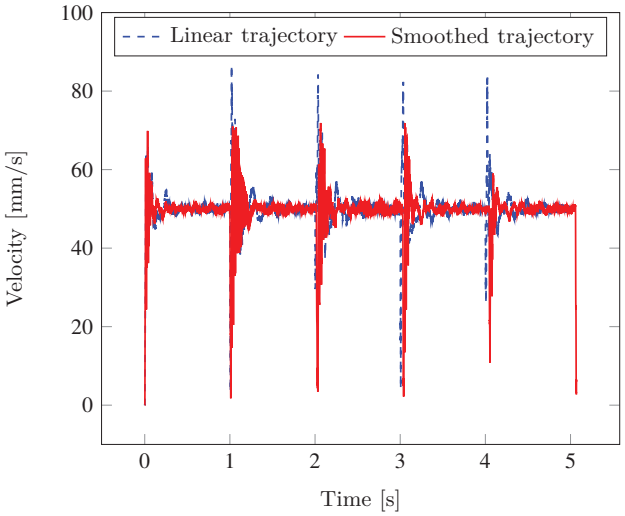

Fig. 11: Experimental results for velocity.

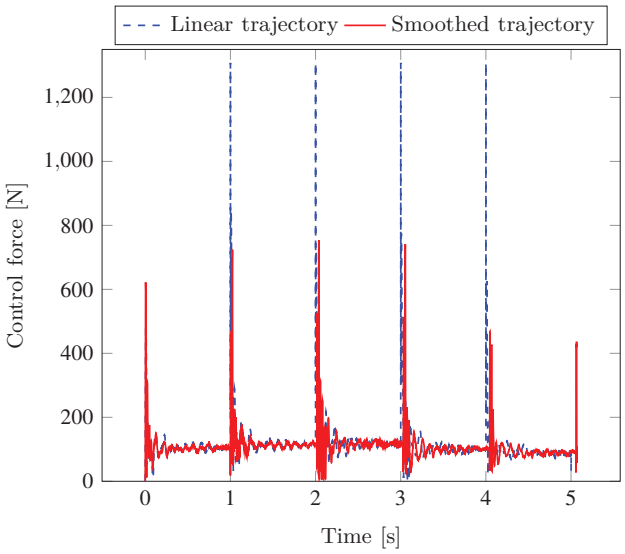

Fig. 12: Experimental input force.

maximum reference velocity was set to $50\,\mathrm{mm\,s^{-1}}$ for both trajectories, the linear trajectory depicts higher overshoots at corners (around 1 s, 2 s, 3 s and 4 s). Similarly for the control forces, the linear trajectory reveals higher requirements with overshoots at corners, as shown in Fig. 12. By integrating the control forces, it was found that the proposed method could reduce the energy consumption by about 8.0 %. On the other hand, the smoothing algorithm has lengthen the cycle time by about 1.36 %.

V. CONCLUSION

This study proposes a simple iterative contouring control and a method to generate smooth trajectories for feed drive systems. The generated trajectories are smooth enough to be tracked by feed drive systems and satisfy kinematic limitations of these systems. In comparison to linear trajectories, experimental results revealed that the proposed trajectories could reduce the maximum contour error by about 61.5 %.

REFERENCES

[1] S. Zhang, "Active vibration control for a flexible string system with input backlash," *IET Control Theory & Applications*, vol. 10, pp. 800–805(5), April 2016.

[2] D. Verscheure, B. Paijmans, H. Van Brussel, and J. Swevers, "Vibration and motion control design and trade-off for high-performance mechatronic systems," *IEEE International Conference on Control Applications*, pp. 1115 – 1120, 2006.

[3] X. Li, H. Zhao, X. Zhao, and H. Ding, "Dual sliding mode contouring control with high accuracy contour error estimation for five-axis cnc machine tools," *International Journal of Machine Tools and Manufacture*, vol. 108, no. Supplement C, pp. 74 – 82, 2016.

[4] M. R. Msukwa, N. Uchiyama, and B. D. Bui, "Adaptive nonlinear sliding mode control with a nonlinear sliding surface for feed drive systems," *IEEE International Conference on Industrial Technology*, pp. 732 – 737, 2017.

[5] M. Hanifzadegan and R. Nagamune, "Contouring control of cnc machine tools based on linear parameter-varying controllers," *IEEE/ASME Transactions on Mechatronics*, vol. 21, pp. 2522–2530, Oct 2016.

[6] A. E. K. Mohammad and N. Uchiyama, "Estimation of tool orientation contour errors for five-axis machining," *Robotics and Computer-Integrated Manufacturing*, vol. 29, no. 5, pp. 271 – 277, 2013.

[7] B. D. Bui, N. Uchiyama, and K. R. Simba, "Contouring control for three-axis machine tools based on nonlinear friction compensation for lead screws," *International Journal of Machine Tools and Manufacture*, vol. 108, pp. 95 – 105, 2016.

[8] K. R. Simba, B. D. Bui, M. R. Msukwa, and N. Uchiyama, "Robust iterative learning contouring controller with disturbance observer for machine tool feed drives," *ISA Transactions*, 2018.

[9] Y. M. Hendrawan, K. R. Simba, and N. Uchiyama, "Embedded iterative learning contouring controller design for biaxial feed drive systems," *International Electronics Symposium*, pp. 37–41, 2016.

[10] K. L. Moore, *Iterative learning control for deterministic systems*. Springer Science & Business Media, 2012.

[11] Z. Yang, L.-Y. Shen, C.-M. Yuan, and X.-S. Gao, "Curve fitting and optimal interpolation for CNC machining under confined error using quadratic B-splines," *Computer-Aided Design*, vol. 66, pp. 62 – 72, 2015.

[12] M. Zhang, W. Yan, C. Yuan, D. Wang, and X. Gao, "Curve fitting and optimal interpolation on CNC machines based on quadratic B-splines," *Science China Information Sciences*, vol. 54, no. 7, pp. 1407 – 1418, 2011.

[13] M. T. Lin, M. C. Lee, J. C. Lee, C. Y. Lee, and Z. W. Jian, "A look-ahead interpolator with curve fitting algorithm for five-axis tool path," *IEEE International Conference on Advanced Intelligent Mechatronics*, pp. 189 – 194, 2016.

[14] T. Theoharis, G. Papaioannou, N. Platis, and N. M. Patrikalakis, *Graphics and Visualization: Principles & Algorithms*. Natick, MA, USA: A. K. Peters, Ltd., 2007.

[15] K. R. Simba, G. Heppeler, B. D. Bui, Y. M. Hendrawan, O. Sawodny, and N. Uchiyama, "Bzier curve based trajectory generation and nonlinear friction compensation for feed drive contouring control," *IFAC-PapersOnLine*, vol. 50, no. 1, pp. 1944 – 1951, 2017.

[16] B. Sencer, K. Ishizaki, and E. Shamoto, "A curvature optimal sharp corner smoothing algorithm for high-speed feed motion generation of NC systems along linear tool paths," *The International Journal of Advanced Manufacturing Technology*, vol. 76, no. 9-12, pp. 1977 – 1992, 2015.

[17] M. Chen, W.-S. Zhao, and X.-C. Xi, "Augmented taylor's expansion method for B-spline curve interpolation for CNC machine tools," *International Journal of Machine Tools and Manufacture*, vol. 94, pp. 109 – 119, 2015.

[18] N. Uchiyama, T. Nakamura, and H. Yanagiuchi, "The effectiveness of contouring control and a design for three-dimensional machining," *International Journal of Machine Tools and Manufacture*, vol. 49, no. 11, pp. 876 – 884, 2009.

[19] K. R. Simba, N. Uchiyama, and S. Sano, "Variable-gain iterative learning contouring control for feed drive systems," *42nd Annual Conference of the IEEE Industrial Electronics Society*, pp. 7227 – 7231, 2016.

[20] M. S. Floater and A. F. Rasmussen, "Point-based methods for estimating the length of a parametric curve," *Journal of Computational and Applied Mathematics*, vol. 196, pp. 512–522, nov 2006.